DOI: 10.61782/fa.2023.0138

forum acusticum 2023

OPTIMISATION OF A MULTI-LAYERED META-PARTITION FOR BROADBAND LOW-FREQUENCY SOUND INSULATION

Kenneth Leung
Institute of Sound and Vibration Research,
University of Southampton
kl3u18@soton.ac.uk

Felix Langfeldt
Institute of Sound and Vibration Research,
University of Southampton
f.langfeldt@soton.ac.uk

ABSTRACT

Acoustic metamaterials, which are usually composed of periodic subwavelength unit cells, are known for their unique capabilities in controlling sound wave propagation. One application of such metamaterials is in using their resonant properties as a lightweight and compact solution to the problematic low frequency range from conventional sound insulation treatments. However, the resonant property of metamaterials only allows for a narrow stopband with superior sound insulation. This paper aims to achieve broadband sound transmission loss in the low frequency range by proposing a multi-layered partition encompassing different metamaterial types. An analytical model of the partition is derived by treating the metamaterial layers with effective material properties inferred from a homogenization method. By applying constraints on the metamaterial and partition properties, such as the overall mass and thickness of the partition, optimizations are then performed to maximize the sound transmission loss within a specific frequency band. A numerical model of the optimized partition is produced to validate the analytical model.

Keywords: *Acoustic Metamaterials, Sound Insulation, Multi-layer Partition, Broadband Low Frequency*

1. INTRODUCTION

Enhancing the low-frequency sound transmission loss (STL) of conventional sound insulating partitions usually requires treatments of additional mass or thickness. However, for applications in the automotive, architectural and aerospace industries, it is challenging to design a performing partition that is also lightweight and compact. In the recent decades, acoustic metamaterials emerged as a solution to provide the superior low-frequency performance that is lacking in conventional sound insulation treatments.

Acoustic metamaterials are composed of subwavelength sized periodic unit cells, known as meta-atoms. They allow the manipulation of sound wave propagation in unprecedented ways, which can be applied in research areas such as acoustic cloaking, acoustic absorption and acoustic lensing [1]. In particular, locally-resonant acoustic metamaterials resonate at frequencies with corresponding wavelengths at orders of magnitude larger than the unit cell size, and can even demonstrate sound insulation properties superior to that from equivalent (in terms of mass or thickness) conventional treatments [2].

This realisation of compact and lightweight acoustic metamaterial designs opened up new possibilities to low-frequency sound control with multi-layered meta-partitions (MLMPs), where metamaterials are incorporated into different layers of conventional sound insulating partitions. Nguyen et al. have shown the use of a double-layer membrane-type acoustic metamaterial as a partition for low-frequency noise control, which had achieved good sound insulation performance between 20 to 59 dB from 320 Hz to 2.5 kHz [3]. Wang et al. introduced an acoustic metamaterial sandwich panel with periodically distributed local resonators constructed of masses positioned on a rubber rod, which showed STL improvements compared to the mass-equivalent sandwich panel without resonators [4]. De Melo Filho et al. designed a lightweight double wall partition consisting of L-shaped vibro-acoustic metamaterials to counteract the STL deficit at the mass-air-mass resonance of a double wall [5]. Langfeldt et al. implemented a double wall partition with a Helmholtz resonator in the air cavity and achieved broadband STL im-

provement through careful tuning of the Helmholtz resonance [6].

There also exists literature looking at applying optimisation methods to maximise sound transmission loss of meta-partitions. Zhang et al. created an optimised lightweight acoustic metamaterial design for low-frequency noise and vibration control of a high-speed train floor [7]. Vazquez Torre et al. applied optimization algorithms to analytical and numerical models of single-layer and double-layer meta-partitions [8].

Much of the literature explores novel designs of multi-layered acoustic meta-partitions using only one meta-atom configuration in a partition to improve broadband STL in the low-frequency regime. Previous work on optimisation of acoustic metamaterials has mainly focused on the design of the meta-atoms and not the partition as a whole. This paper aims to bridge the gaps by designing and optimising a meta-partition containing more than one meta-atom type.

The paper is organised as followed. Firstly, an analytical model of a multi-layer meta-partition is defined from an expansion of a double wall partition formula and representing the metamaterial layers with effective material properties. Following this, the optimisation problem is outlined, with the results described and discussed with relations to the underlying physics. Next, the chosen optimal design is simulated in a numerical model to compare with results from the analytical model. Finally, all the findings and analysis are summarised in the conclusions.

2. ANALYTICAL MODEL

This section first considers a double wall partition, a conventional multi-layered solution for sound insulation treatments. Their transmission characteristics at normal incidence can be calculated analytically using the transmission coefficient [9]

$$\tau_{\text{double}} = \left|\left(1 + (X_1 + X_2) + X_1 X_2 \left(1 - e^{-2\mathrm{j}kd}\right)\right)\right|^{-2}, \tag{1}$$

where $X_{1,2} = \mathrm{j}\omega\rho_{1,2}d_{1,2}/(2\rho_0 c_0)$ are the normalised impedance of the wall 1 and wall 2 of the double wall partition, respectively. $\rho_{1,2}$ are the mass densities of each wall, $d_{1,2}$ are the thicknesses of each wall, ρ_0 and c_0 are the density and speed of sound of air, d is the air gap layer thickness, and $k = \omega/c_0$ is the acoustic wavenumber, where $\omega = 2\pi f$ is the circular frequency with f as frequency. It is more common to represent sound insulation with the sound transmission loss (TL), which is obtained with

$$\mathrm{TL} = 10 \log \frac{1}{\tau}. \tag{2}$$

The typical STL profile of a double wall partition has superior performance at higher frequencies in comparison to a single wall partition with the same mass. For lower frequencies, the STL is identical to that of an equivalent single wall, where the partition performance is mainly dependent on its mass. The frequency separating these two regions is known as the mass-air-mass frequency f_{MAM},

$$f_{\text{MAM}} = \frac{c_0}{2\pi}\sqrt{\frac{\rho_0(\rho_1 d_1 + \rho_2 d_2)}{d\rho_1 d_1 \rho_2 d_2}}, \tag{3}$$

which is known to have a deficit in STL due to the resonant behaviour of the system. Therefore, conventional noise control treatments aim to reduce the mass-air-mass frequency as low as possible. However, Eqn. (3) shows that the thickness and the mass of the partition have to be increased to reduce f_{MAM}, which would not result in a lightweight and compact solution. Acoustic metamaterials offer the solution to not only correct the the STL deficit at f_{MAM}, but also increase the general performance at the low frequency regime below f_{MAM}. The multi-layered meta-partition considered in this paper contains mass-spring resonators on the partition walls and a Helmholtz resonator in the air gap. To quantify the effect of the metamaterials on the double wall performance, each layer of the partition is treated as a homogeneous medium with effective parameters such as the effective mass density and bulk modulus. This is known as the effective medium theory [1].

The effect of attaching periodic mass-spring resonators to the walls results in a frequency-dependent effective mass density of each wall meta-layer. This quantity is expressed as $\rho_{\text{eff}1,2}$ and can be calculated by

$$\rho_{\text{eff}1,2} = \rho_{1,2}d_{1,2} + \frac{m_{1,2}}{S}\left[\frac{\frac{2\mathrm{j}\zeta_{1,2}\omega}{\omega_{1,2}} + 1}{1 + \frac{2\mathrm{j}\zeta_{1,2}\omega}{\omega_{1,2}} - \frac{\omega^2}{\omega_{1,2}^2}}\right], \tag{4}$$

where S is the surface area of the unit cell, $m_{1,2}$ are the moving masses of the resonators, $\zeta_{1,2}$ are the damping ratios of the resonators, and $\omega_{1,2}$ are the circular natural frequencies of the resonators on each wall respectively [5].

When placed in between the walls of a double wall, Helmholtz resonators have been shown to influence the bulk modulus of the air gap. Assuming the fluid within both the Helmholtz resonator and the air gap to have the

same bulk modulus K_0, the effective bulk modulus K_{eff} of a Helmholtz resonator-based acoustic metamaterial is expressed as [6]

$$K_{\text{eff}} = \frac{K_0}{1 - \phi_{\text{hr}} + \frac{\phi_{\text{hr}}}{1 + 2\text{j}\zeta_{\text{hr}}\Omega_{\text{hr}} - \Omega_{\text{hr}}^2}}. \tag{5}$$

In Eqn. (5), the Helmholtz resonator resonance frequency is written as a ratio $\Omega_{\text{hr}} = f/f_{\text{hr}}$, where f_{hr} is the Helmholtz resonance frequency. The effective bulk modulus is also dependent on the volumetric filling ratio $\phi_{\text{hr}} = V_{\text{hr}}/V$, which is defined to be the ratio between the resonator volume V_{hr} to the total volume of the air gap in each unit cell V. ζ_{hr} is the damping coefficient of the resonator accounting for thermoviscous losses from the vibrating air column in the neck of the Helmholtz resonator. The presence of the Helmholtz resonator also increases the overall fluid density by [6]

$$\rho_{\text{eff}} \approx \rho_0 \frac{2 + \phi_{\text{hr}}}{2(1 - \phi_{\text{hr}})}. \tag{6}$$

Putting equations (4), (5) and (6) together into Eqn. (1) gives the analytical result for the transmission coefficient of a multi-layered meta-partition (MLMP):

$$\tau_{\text{MLMP}} = \left| \frac{2Z_{\text{MLMP}} \sin(k_{\text{eff}} d)}{X_{\text{MLMP1}} X_{\text{MLMP2}} \sin^2(k_{\text{eff}} d) + Z_{\text{MLMP}}^2} \right|^2, \tag{7}$$

where $Z_{\text{MLMP}} = Z_{\text{eff}}/(\rho_0 c_0)$, $X_{\text{MLMP1,2}} = X_{\text{norm1,2}} + 1 - \text{j}Z_{\text{MLMP}} \cot(k_{\text{eff}} d)$ and $X_{\text{norm1,2}} = \text{j}\omega\rho_{\text{eff1,2}}/(\rho_0 c_0)$ are the normalised wall impedances of the two walls. $Z_{\text{eff}} = \sqrt{K_{\text{eff}}\rho_{\text{eff}}}$ and $k_{\text{eff}} = \omega\sqrt{\rho_{\text{eff}}/K_{\text{eff}}}$ are the effective impedance and wavenumber of the air gap layer, respectively. Eqn. (2) is used to calculate the sound transmission loss of the MLMP, using τ_{MLMP} in place of τ.

3. OPTIMISATION

With the analytical model for the sound transmission loss of the multi-layered meta-partition described above, a constrained single-objective optimisation problem is formulated to maximise the partition's performance:

$$\text{Maximise} \int_{100\,\text{Hz}}^{500\,\text{Hz}} \min(\text{TL}_{\text{MLMP}}(f) - \text{TL}_{\text{ref}}(f), 6\,\text{dB})\,\text{d}f$$

subject to

$$\begin{aligned} & d_1 + d + d_2 \leq 100\,\text{mm} \\ & \rho_1 d_1 + \frac{m_1}{S} + \rho_2 d_2 + \frac{m_2}{S} \leq 5\,\text{kg}\,\text{m}^{-2}, \end{aligned} \tag{8}$$

where TL_{MLMP} is the sound transmission loss of the MLMP and TL_{ref} is the sound transmission loss a double wall partition with equivalent mass and thickness.

The objective function, as described in Eqn. (8), evaluates the improvement of the MLMP by taking the difference of its sound transmission loss to that of the equivalent double wall across a range of frequencies. For this optimisation problem, the frequency range of interest is set from 100 to 500 Hz. The integral is approximated using the trapezoidal numerical integration method. A 6 dB upper limit is imposed in the integrand to disregard regions of sharp resonances and encourage a broadband STL solution. A linear constraint for the overall thickness of the partition is posed at 100 mm and a nonlinear constraint for the mass of the partition of 5 kg m^{-2} is set for a compact and lightweight solution.

15 design variables are used in this optimisation problem, which consist of parameters that relate to the partition itself as well as to the metamaterials. These design variables are selected as they can be easily substituted into the equations in section 2, and provide enough geometrical and acoustical parameters to tackle this optimisation problem. The design variables are outlined in Tab. 1 along with their lower and upper bounds. The optimization is performed on MATLAB with fmincon, a nonlinear programming solver, which implements the interior-point method to search for the solution. Various runs of the optimisation algorithm with randomized initial conditions were carried out to increase the likelihood that the global maximum of the optimisation problem is found.

The sound transmission loss of the optimised multi-layered meta-partition is shown in Fig. 1, and the optimised values of the design parameters are shown in Tab. 2. In general, there is a broadband sound transmission loss improvement of the multi-layer meta-partition in comparison to a double wall with equivalent mass. The resonance frequencies, which occur at 100 Hz, 139 Hz and 247 Hz, are spaced relatively far from one another within the frequency range of interest to increase the bandwidth for STL improvement. However, the higher frequencies of the meta-partition are performing worse than the double wall. This behaviour is likely a result from the resonant properties of the wall mass-spring resonators, and is further analysed and discussed below.

To better understand the effect of each metamaterial layer on the meta-partition, variations of the optimised meta-partition with only one layer of metamaterials are plotted in Fig. 2. From the figure, the resonator on wall 1 plays the dominant role on the STL performance of the

Table 1. Optimisation problem design variables along with lower and upper bounds.

Design Variable	Symbol	Lower Bound	Upper Bound	Unit
Unit Cell Area	S	10^{-4}	$c_0/(10f_{\max})$	m^2
Wall 1 Density	ρ_1	170	11340	$\mathrm{kg\,m}^{-3}$
Wall 1 Thickness	d_1	10^{-4}	$d_{\mathrm{tot}}/2$	m
Wall 1 Resonator Mass	m_1	10^{-6}	10^{-4}	kg
Wall 1 Resonator Frequency	f_1	100	500	Hz
Wall 1 Resonator Damping Ratio	ζ_1	10^{-3}	0.5	
Air Gap Width	d	10^{-2}	$d_{\mathrm{tot}}/2$	m
Helmholtz Resonator Volumetric Ratio	ϕ_{hr}	0.1	0.6	
Helmholtz Resonator Frequency	f_{hr}	100	500	Hz
Helmholtz Resonator Damping Ratio	ζ_{hr}	10^{-3}	0.5	
Wall 2 Density	ρ_2	170	11340	$\mathrm{kg\,m}^{-3}$
Wall 2 Thickness	d_2	10^{-4}	$d_{\mathrm{tot}}/2$	m
Wall 2 Resonator Mass	m_2	10^{-6}	10^{-4}	kg
Wall 2 Resonator Frequency	f_2	100	500	Hz
Wall 2 Resonator Damping Ratio	ζ_2	10^{-3}	0.5	

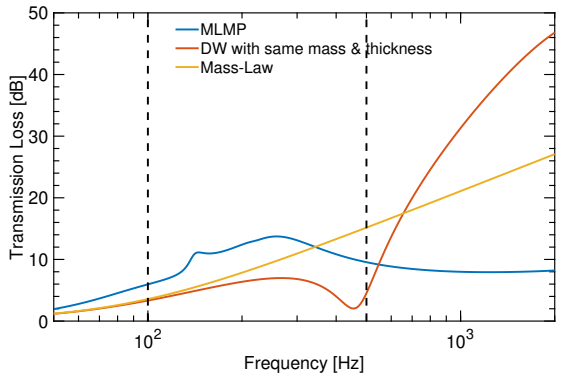

Figure 1. Sound transmission loss of the optimised multi-layered meta-partition. The optimised meta-partition is plotted in blue whereas a double wall with equivalent mass is plotted in red. The equivalent mass-law is plotted in yellow.

meta-partition, particularly at frequencies above approx. 200 Hz. The resonator on the second wall mainly contributes in the lower frequency region up to its resonance frequency of 100 Hz. The spread of the resonance frequencies from the wall resonators allows for the STL improvement from 100 - 500 Hz, as seen with the yellow curve in Fig. 2, which even performs better than the optimised MLMP at higher frequencies (in blue).

The mass-spring resonators on the walls introduce a complex relationship between frequency and the partition's mass-air-mass resonance [5]. For this optimised partition, the mass-air-mass resonance is shifted to a higher frequency. This introduces a region above the mass-spring resonance frequency where the STL performance decreases, despite the increase in STL performance of the mass-equivalent double wall in Fig. 1.

The Helmholtz resonator-type acoustic metamaterial contributes mainly to the lower frequency STL region below its resonance at approx. 200 Hz. This leads to a broader improvement bandwidth for the optimised MLMP. However, this bandwidth increase in the lower frequency sacrifices performance in the higher frequency region beyond approx. 300 Hz, which is likely due to the decoupling of the fluid within the Helmholtz resonator with the surrounding air gap layer.

The optimised value of the surface area of the unit cell

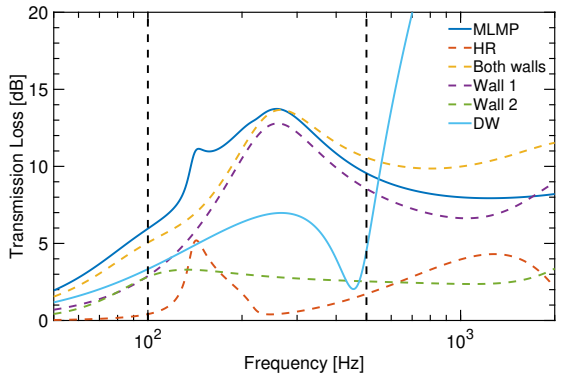

Figure 2. Sound transmission loss of variations in the optimised meta-partition. The optimised partition is in blue, the variation with only the Helmholtz resonator in red, the variation with wall resonators is in yellow, and the variations with resonators only on one of the walls are in purple and green. The reference double-walled partition with equivalent mass and thickness is shown in light blue.

(100 mm^2), assuming the unit cells to be square shaped, would lead to an edge length of 10 mm. This was an interesting result as the optimised value was extremely close to the lower boundary in the optimisation problem, and is generally smaller compared to the unit cells typically used in the literature with edge lengths of 30 to 60 mm [4, 10]. The resulting densities of both walls are extremely small at 170 kg m^{-3} and 264 kg m^{-3}, which is quite close to the density of light wood materials such as Balsa wood. The optimisation problem also resulted in relatively thin wall layers, which were in the order of 0.1 mm. Similar to the unit cell surface area, these optimised results were very close to the lower boundary. Some literature have shown partitions with thin wall layers, such as the middle wall layer of Lin's meta-partition (0.2 mm), constructed using Polyethylene terephthalate (PET) of density 1450 kg m^{-3} [11]. However, the outer layers were still 2 mm thick, which raises the questions if the outer wall layers of the optimized meta-partition should not be too thin for practical use.

Most of the other design parameters, such as the masses of the resonators and Helmholtz resonator related parameters, look like reasonable results. In particular, the optimised air gap layer at 50 mm is typical in current literature on meta-partitions, which are typically tens of millimeters thick [3]. However, the damping values of the mass-spring resonators are much higher than damping ratios found in conventional treatments and other metamaterials. For example, de Melo Filho et al. used a damping ratio of 2 % for their mass-spring metamaterial [5], which is more than a factor of 10 smaller than the damping ratio values obtained in the optimisation.

Table 2. Optimised design parameters of the MLMP.

Design Variable	Optimised Value	Unit
S	0.0001	m^2
ρ_1	170.50	kg m^{-3}
d_1	0.00010	m
m_1	10^{-4}	kg
f_1	247.11	Hz
ζ_1	0.32	
d	0.050	m
ϕ_{hr}	0.60	
f_{hr}	139.01	Hz
ζ_{hr}	0.05	
ρ_2	263.92	kg m^{-3}
d_2	0.00010	m
m_2	4.41×10^{-5}	kg
f_2	100.00	Hz
ζ_2	0.50	

One possible reason that a few design variables had optimised values near their boundaries could be that the optimisation algorithm was converging to a local minimum. Further work could be done by investigating this problem with different optimisation algorithms, such as genetic algorithms, to search for possible better performing partition solutions.

4. NUMERICAL MODEL VERIFICATION

The performance of the optimised multi-layer meta-partition is evaluated with finite element analysis using COMSOL Multiphysics. Taking our optimised values, a single unit cell of the partition is modelled with periodic boundary conditions to simulate an infinitely large sample. Each of the walls are modelled using shell elements.

The wall resonators are modelled as cylinder-shaped resonators with a tungsten upper layer and a rubber lower layer. The stiffness of the wall resonators $s_{1,2}$ is estimated using

$$s_{1,2} = \frac{E\pi r_{s1,2}^2}{h_{s1,2}}, \tag{9}$$

where $E = 150\,\mathrm{kPa}$ is the Young's modulus of the rubber material and $r_{s1,2}$ and $h_{s1,2}$ are the radius and height of the cylindrical resonator stiffness layer, respectively [4]. The thickness of the mass layer $h_{m1,2}$ is derived using

$$h_{m1,2} = \frac{m_{1,2}}{(\rho_{m1,2}\pi r_{m1,2}^2)}, \tag{10}$$

where $\rho_{m1,2} = 19\,250\,\mathrm{kg\,m^{-3}}$ is the density of tungsten and $r_{m1,2}$ is the radius of the cylindrical resonators. Using Eqn. (9) and Eqn. (10) with the natural frequency of a single degree-of-freedom oscillator

$$f_{1,2} = \frac{1}{2\pi}\sqrt{\frac{s_{1,2}}{m_{1,2}}}, \tag{11}$$

the stiffness and mass layer heights for each resonator can be adjusted to tune the resonator to the desired resonance frequencies $f_{1,2}$. Having encountered issues with viscous damping modelling in COMSOL, a loosely equivalent isotropic loss factor was assumed for the resonators.

The Helmholtz resonator is modelled with negligible wall thickness and mass in the air gap, with its walls modelled as interior sound hard boundaries. The resonance frequency f_{hr} of the resonator can be related to the geometry of the Helmholtz resonator by

$$f_{\mathrm{hr}} = \frac{c_0}{2\pi}\sqrt{\frac{A_{\mathrm{n}}}{V_{\mathrm{hr}}L_{\mathrm{n,eff}}}}, \tag{12}$$

where $A_{\mathrm{n}} = \pi r_{\mathrm{n}}^2$ is the cross-sectional area of the Helmholtz resonator neck, r_{n} is the neck radius and $L_{\mathrm{n,eff}} = L_{\mathrm{n}} + 1.7r_{\mathrm{n}}$ is the effective Helmholtz resonator neck length, accounting for end correction effects and L_{n} being the actual length of the Helmholtz resonator neck. Given that the Helmholtz resonator body volume is fixed with the volumetric ratio, the Helmholtz resonator neck length and cross-sectional area are tuned with Eqn. (12) to maintain the resonator's resonance frequency. In the simulation model, narrow region acoustics physics are applied to simulate the Helmholtz resonator damping, which is inversely proportional to the neck radius. The design of the resonators that was implemented in the numerical model can be seen in Fig. 3.

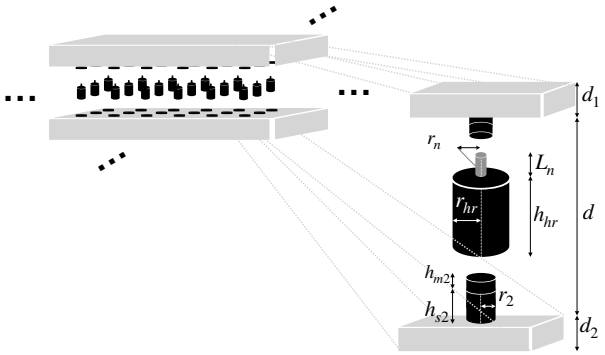

Figure 3. Sketch of the numerical model of the multi-layered meta-partition consisting of cylindrical wall mass-spring resonators and Helmholtz resonators within the air gap.

The sound transmission loss of the multi-layered meta-partition from the numerical model is compared to that of the analytical model in Fig. 4. The simulated STL values loosely verify the analytical model. At lower frequencies, the results generally agree amongst both models, however the behaviour differs towards the higher frequencies. There was also difficulty in determining the damping of the Helmholtz resonator, where the Helmholtz resonator peak is missing from the numerical model results. The differences between the models are likely due to a few different assumptions and definitions, which are discussed below.

One source of the difference between the numerical and analytical models would be in the stiffness approximation of the wall resonators using Eqn. (9), which only accounted for axial stresses. To correctly calculate the stiffness of the mass-spring resonators, one would have to include additional terms relating to the Poisson's ratio to account for stresses in the other two directions. To reduce the error in the STL from this issue, minor tweaking to the stiffness and mass layer thickness were attempted to match the resonance frequencies between the two models to produce the results in Fig. 4

The next assumption is that the analytical model only considered mass-spring resonators with one resonance frequency, whereas the cylindrical resonators in the numerical model exhibit higher order resonances and anti-resonances. In Fig. 4, the performance of the numerical model is consistently below the analytical STL between

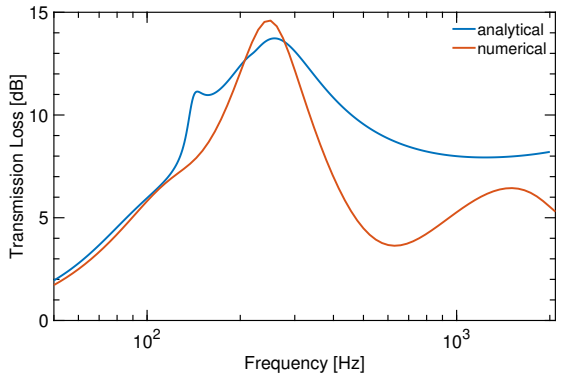

Figure 4. Comparison of the sound transmission loss of the optimised multi-layered meta-partition from the analytical model (in blue) and the numerical model (in red).

300 Hz to 1500 Hz, and particularly there are dips in STL performance at approximately 500 Hz and 1 kHz. After inspection of the numerical results, these dips are resulting from anti-resonance frequencies of the wall 1 resonator, which leads to increased sound transmission through the partition and was unaccounted for in the analytical model.

One particular difference is the deficit STL performance of the numerical model at higher frequencies (above approx. 300 Hz) compared to that of the analytical model. Initial inspections in the numerical results show that poor STL performances occurs in particular for the wall resonator layers in this frequency region. There has yet to be an explanation yet to this difference between the analytical and numerical models, and this discrepancy would be further investigated in future work.

Despite qualitative similarities between all the models near the wall mass-spring resonator resonances, there are slight differences due to the use of different damping models. The matching of the viscous damping ratio in the analytical model $\zeta_{1,2}$ to the isotropic loss factor in the computational model $\eta_{1,2}$ was applied with the relation $\eta_{1,2} = 2\zeta_{1,2}$, but this relationship only holds true at the resonance frequencies. In fact, the viscous damping yields higher STL results compared to the loss factor damping above resonance and the opposite occurs below resonance. However, there seems to remain some mismatch in the damping of the peaks of the wall 1 resonator (with the resonance frequency at 247 Hz, which is another area for further work.

The damping of the Helmholtz resonator was also difficult to realise. Attempts at changing the Helmholtz resonator neck radius were made to match the damping of the Helmholtz resonator in the numerical model to the value used in the analytical model. However, the resulting Helmholtz resonator had a thin neck in order to tune the resonance frequency of the Helmholtz resonator to f_{hr} with Eqn. (12) and allow it to fit within the air gap. Having restricted the dimensions of the neck radius, the Helmholtz resonator modelled in COMSOL was overdamped. This resulted in a deficit in contribution to the overall STL between 100 Hz to 200 Hz, where the peak occurs for the blue curve but not for the red curve in Fig. 4.

A practicality factor that was not considered in this optimisation problem were the walls of the Helmholtz resonators. In this work, the walls were modelled as rigid boundaries. However, realistically the resonator walls would have finite thickness, stiffness and mass, which would contribute to the total mass constraint of the optimisation problem. Similarly, the cylindrical resonators on the resonator walls only have taken into account the mass of the tungsten layer, and it would be a more complete optimisation problem to also consider the mass of the stiffness layers.

5. CONCLUSIONS

In summary, this paper proposes a design of a multi-layered meta-partition aiming at a broadband sound transmission loss improvement compared to a conventional double-wall with equivalent mass. Effective homogeneous fluid theory was applied for the effect of mass-spring resonators on the walls along with a Helmholtz resonator in the air gap to estimate the performance of the partition analytically. A single-objective constrained optimisation problem was designed and implemented to maximize the broadband STL of the partition. The optimised partition is realised with a numerical model for verification purposes.

The optimization results showed that there is a broadband STL improvement of the multi-layered meta-partition in comparison to the equivalent mass double wall, which was due to the spread of resonances from the metamaterials to expand the bandwidth of STL improvement. However, the dominating mass density behaviour from the wall mass-spring resonators resulted in a shift of the mass-air-mass resonance to higher frequencies, which

resulted in the lack of higher frequency performance in comparison to the mass-equivalent double wall.

The numerical simulations results generally agreed with the analytical model results. However, few assumptions, including the modelling of the mass-spring resonators and damping of all the metamaterials, resulted in differences. The higher frequency region above 300 Hz also exhibited greater differences between the analytical and numerical models. The reason for these differences will be further explored in future work.

Generally, the optimised design parameter values are practical and consistent with literature, with few deviations including a smaller unit cell size, a thinner wall thickness, as well as larger than typical damping values. This led to some aspects of the partition to not be very realisable.

The results in this paper have shown promise in using different meta-layers to achieve a multi-layered partition with broadband STL improvement. Some further work could include using conventional sound absorbing treatments to improve the STL at higher frequencies, as explored in other literature [12]. Additionally, the optimisation algorithm could be revisited to give more realisable solutions, which could hopefully lead to better agreement between the analytical and numerical models. Lastly, the natural progression from this paper is to continually add more meta-layers to the meta-partition, and investigate the trade-offs of STL performance with practicality aspects such as the partition weight and compactness with multi-objective optimisation.

6. REFERENCES

[1] G. Liao, C. Luan, Z. Wang, J. Liu, X. Yao, and J. Fu, "Acoustic metamaterials: a review of theories, structures, fabrication approaches, and applications," *Advanced Materials Technologies*, vol. 6, p. 2000787, May 2021.

[2] Z. Yang, J. Mei, M. Yang, N. H. Chan, and P. Sheng, "Membrane-type acoustic metamaterial with negative dynamic mass," *Physical Review Letters*, vol. 101, p. 204301, Nov. 2008. Publisher: American Physical Society.

[3] H. Nguyen, Q. Wu, J. Chen, Y. Yu, H. Chen, S. Tracy, and G. Huang, "A broadband acoustic panel based on double-layer membrane-type metamaterials," *Applied Physics Letters*, vol. 118, p. 184101, May 2021.

[4] S. Wang, X. Zhang, F. Li, and S. M. Hosseini, "Sound transmission loss of a novel acoustic metamaterial sandwich panel: Theory and experiment," *Applied Acoustics*, vol. 199, p. 109035, Oct. 2022.

[5] N. G. R. de Melo Filho, L. Van Belle, C. Claeys, E. Deckers, and W. Desmet, "Dynamic mass based sound transmission loss prediction of vibro-acoustic metamaterial double panels applied to the mass-air-mass resonance," *Journal of Sound and Vibration*, vol. 442, pp. 28–44, Mar. 2019.

[6] F. Langfeldt, H. Hoppen, and W. Gleine, "Broadband low-frequency sound transmission loss improvement of double walls with helmholtz resonators," *Journal of Sound and Vibration*, vol. 476, p. 115309, June 2020.

[7] J. Zhang, D. Yao, W. Peng, R. Wang, J. Li, and S. Guo, "Optimal design of lightweight acoustic metamaterials for low-frequency noise and vibration control of high-speed train composite floor," *Applied Acoustics*, vol. 199, p. 109041, Oct. 2022.

[8] J. H. Vazquez Torre, J. Brunskog, V. Cutanda Henriquez, and J. Jung, "Hybrid analytical-numerical optimization design methodology of acoustic metamaterials for sound insulation," *The Journal of the Acoustical Society of America*, vol. 149, pp. 4398–4409, June 2021.

[9] A. London, "Transmission of reverberant sound through double walls," *The Journal of the Acoustical Society of America*, vol. 22, pp. 270–279, Mar. 1950.

[10] D. Roca, J. Cante, O. Lloberas-Valls, T. Pàmies, and J. Oliver, "Multiresonant layered acoustic metamaterial (mlam) solution for broadband low-frequency noise attenuation through double-peak sound transmission loss response," *Extreme Mechanics Letters*, vol. 47, p. 101368, Aug. 2021.

[11] Q. Lin, Q. Lin, Y. Wang, and G. Di, "Sound insulation performance of sandwich structure compounded with a resonant acoustic metamaterial," *Composite Structures*, vol. 273, p. 114312, Oct. 2021.

[12] G. Kyaw Oo D'Amore, S. Caverni, M. Biot, G. Rognoni, and L. D'Alessandro, "A metamaterial solution for soundproofing on board ship," *Applied Sciences*, vol. 12, p. 6372, Jan. 2022. Number: 13 Publisher: Multidisciplinary Digital Publishing Institute.